A three level finite element approximation of a pattern formation model in developmental biology

Marcus R. Garvie & Catalin Trenchea

Numerische Mathematik

ISSN 0029-599X

Numer. Math.
DOI 10.1007/s00211-013-0591-z

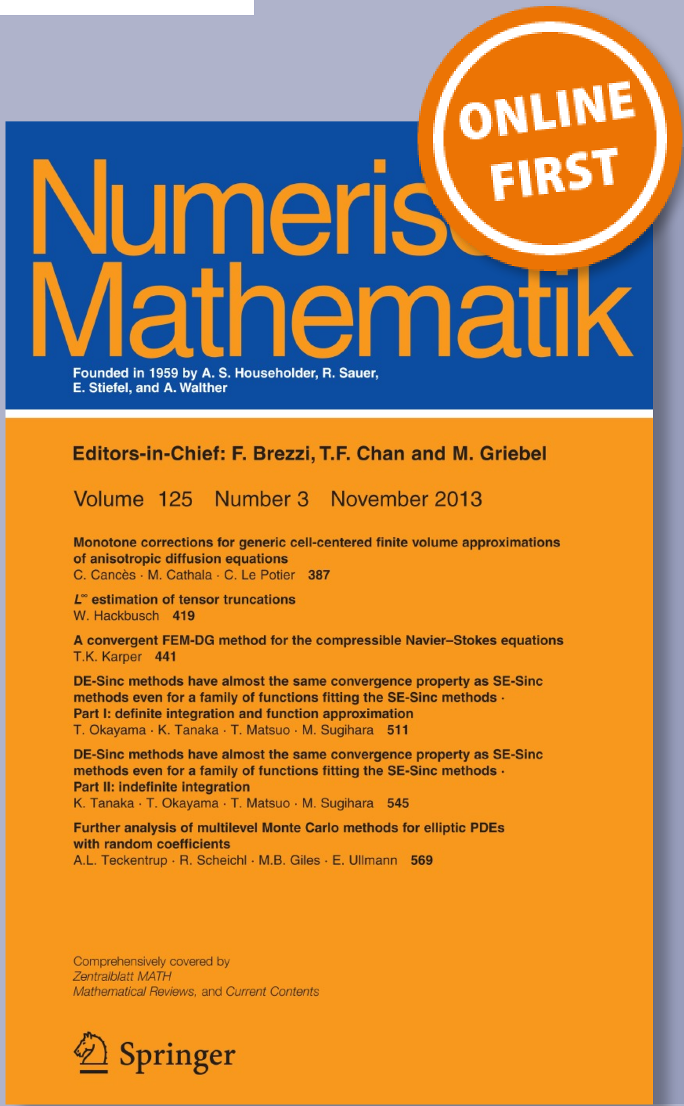

Springer

Numer. Math.
DOI 10.1007/s00211-013-0591-z

Numerische Mathematik

A three level finite element approximation of a pattern formation model in developmental biology

Marcus R. Garvie · Catalin Trenchea

Received: 24 September 2012 / Revised: 5 July 2013

Abstract This paper concerns a second-order, three level piecewise linear finite element scheme 2-SBDF (Ruuth, in J Math Biol 34:148–176, 1995) for approximating the stationary (Turing) patterns of a well-known experimental substrate-inhibition reaction-diffusion ('Thomas') system (Thomas, in Analysis and control of immobilized enzyme systems, pp 115–150, 1975). A numerical analysis of the semi-discrete in time approximations leads to semi-discrete a priori bounds and an optimal error estimate. The analysis highlights the technical challenges in undertaking the numerical analysis of multi-level ($\geq$3) schemes. We illustrate the effectiveness of the numerical method by repeating an important classical experiment in mathematical biology, namely, to approximate the Turing patterns of the Thomas system over a schematic mammal skin domain with fixed geometry at various scales. We also make some comments on the correct procedure for simulating Turing patterns in general reaction-diffusion systems.

Mathematics Subject Classification 35K57 · 65N30 · 65M15 · 92C15

1 Introduction and motivation

In this paper we study the numerical solutions of a two-component reaction-diffusion system of Thomas [58], which after non-dimensionalization [46] has the following form:

M. R. Garvie (✉)
Department of Mathematics and Statistics, University of Guelph, Guelph, ON N1G 2W1, Canada
e-mail: mgarvie@uoguelph.ca

C. Trenchea
Department of Mathematics, University of Pittsburgh, Pittsburgh, PA 15260, USA
e-mail: trenchea@pitt.edu

Published online: 01 November 2013

$$\begin{cases} \frac{\partial u}{\partial t} = \Delta u + a - u - h(u, v), \\ \frac{\partial v}{\partial t} = \delta \Delta v + \alpha(b - v) - h(u, v), \\ h(u, v) = \frac{\rho u v}{1+u+Ku^2}. \end{cases} \tag{1.1}$$

Here $u(\mathbf{x}, t)$ and $v(\mathbf{x}, t)$ are morphogen concentrations at time t and (vector) position $\mathbf{x}$. Δ is the Laplacian operator in two space dimensions, and the parameters $\delta,\ \alpha,\ a,\ b,\ \rho$, and K are strictly positive. We assume homogeneous Neumann boundary conditions and appropriate initial data (additional details given below).

System (1.1) is a popular reaction-diffusion system for studying pattern formation and has been used to investigate the mechanisms governing the differentiation and growth of the structure of an organism ('morphogenesis') [6,44–47]. In addition to these studies, researchers have carried out: a non-linear stability analysis using a multi-scale perturbation method [49]; a mathematical analysis and numerical study of the Thomas system with time delay [51]; and a study of the long-time behaviour of the Thomas system with Robin boundary conditions [54].

Complex systems with interacting components frequently give rise to 'emergent properties', or pattern formation phenomena. The study of models in nature for pattern formation is an intensive area of research. Examples include the distribution of plankton in the ocean [42], morphogenesis of organisms [60], chemotaxis [34], and cardiac arrhythmias [31], to cite just a few. A large number of pattern formation phenomena, including those cited above, can be modeled by the Turing [60] mechanism in reaction-diffusion systems. Turing demonstrated that for appropriate conditions on the reaction kinetics and distinct diffusion coefficients, systems of two or more chemical species can react and diffuse to produce spatially heterogeneous solutions, namely, a spatial pattern. This phenomena is also known as 'diffusion-driven instability', as in the spatially homogeneous situation there is a linearly stable equilibrium solution that can become linearly unstable in the presence of diffusion. The applicability of the Turing mechanism to interacting ecological species was first shown in [36]. For additional background material on pattern formation in biology see [41,47].

Many reaction-diffusion systems have been used to investigate morphogenesis in the Turing sense, however the precise mechanisms responsible for pattern formation in embryonic development are still unknown. Murray [46] showed that the major difference between them are in the parameter ranges for diffusion driven instability ('Turing Space'), and that the Thomas system possesses the largest Turing Space among the practical systems [46].

The effective numerical approximation of reaction-diffusion equations for pattern formation requires special treatment. Consider a generic system of reaction diffusion equations of the form

$$\mathbf{w}_t = D\Delta\mathbf{w} + \mathbf{f}(\mathbf{w}), \tag{1.2}$$

where $\mathbf{w}$ is the vector of chemical concentrations, $\mathbf{f}$ is the vector of nonlinear reaction kinetics and D is a diagonal matrix of diffusion coefficients. Assume that (1.2) has been discretised in space, e.g. by the finite element or finite difference method, to give a system of ordinary differential equations of the form

$$\dot{\mathbf{W}} = D\Delta_h \mathbf{W} + \mathbf{F}(\mathbf{W}), \tag{1.3}$$

where $\mathbf{F}(\mathbf{W})$ and $\Delta_h \mathbf{W}$ arise from the approximation of the reaction kinetics and the diffusion terms respectively, and Δ_h is the discrete Laplacian operator. Many time stepping schemes have been proposed for the approximation of (1.3) (see e.g. [59] for an introduction). For example, the Backward Euler scheme (e.g., [22]), the Crank–Nicolson method (e.g., [19]), Runge-Kutta methods (e.g., [39]) and various semi-implicit (linear) solvers (e.g., [28]) have been effectively employed in the 2-component case. Ruuth [55] (cf. [7]) analyzed the performance of several linear multistep implicit-explicit (IMEX) schemes for reaction-diffusion equations in pattern formation, and found that some popular first-order schemes, as well as schemes that lead to weak decay of high frequency spatial errors, may yield plausible results that are qualitatively incorrect. Ruuth recommends a second-order IMEX scheme with strong decay of high frequency errors, namely, the semi-implicit backward differentiation formula (2-SBDF) given by

$$\frac{1}{2\Delta t}\left(3\mathbf{W}^{n+1} - 4\mathbf{W}^{n} + \mathbf{W}^{n-1}\right) = D\Delta_h \mathbf{W}^{n+1} + 2\mathbf{F}(\mathbf{W}^{n}) - \mathbf{F}(\mathbf{W}^{n-1}). \tag{1.4}$$

This scheme has also been referred to in the literature as 'Extrapolated Gear' (see [61] and others). As this scheme has three time levels, in addition to an initial approximation $\mathbf{W}^0$, the time stepping procedure requires an approximation at the first step, namely $\mathbf{W}^1$. One way to kick-start this procedure is to use a first-order IMEX scheme, for example 1-SBDF [55].

There are numerous works on multistep finite element methods, many of which are of the IMEX type. Some early works concerned finite element multistep methods for linear parabolic problems [11,43,63], or were concerned with linear stability analysis [7,26,61]. Multistep finite element methods of the IMEX type have been applied to various problems, for example, the nonlinear Schrödinger equation [12], the approximation of Turing patterns in electrodeposition [56], the Gray–Scott model for pattern formation [62], the Kuramoto–Sivashinsky equation [4], nonlinear Convection–Diffusion problems [13], the propagation of electrical potential waves in the myocardium [25], semiconductor devices [14–16], and a paper with applications to the spatial discretization of the Stokes–Darcy problem [35]. A few papers specifically concern the 2-SBDF scheme [7,12,40,55,56], however, none provide rigorous stability and error estimates for this time-stepping scheme coupled with the finite element method for solving nonlinear parabolic PDEs. For a general theoretical framework for proving abstract convergence results for multistep IMEX schemes applied to various nonlinear parabolic problems see [1–3]. The methodology relies on appropriate stability and consistency conditions and was successfully applied in [62] to obtain optimal error estimates for the Gray–Scott model. Another numerical analysis study [23] analysed the temporal discretization of semilinear parabolic problems in an abstract setting by the two-step backward differentiation formula with variable time steps. With equal time steps the approximation of the time derivative is the same as in the 2-SBDF scheme, however the right hand side of the scheme has the form $\mathbf{F(W^n)}$ (cf. (1.4)). Stability as well as optimal smooth data error estimates are derived assuming adjacent time steps do not differ by too much. We also mention a paper [38] that develops a family of multistep IMEX predictor–corrector schemes for approximating nonlinear Parabolic PDEs. The numerical methods are efficient and possess larger stability regions than earlier IMEX schemes, however an error analysis is lacking. For additional references on IMEX and multistep schemes for the numerical solution of advection–reaction–diffusion PDEs see the comprehensive research monograph [33].

The main aim of this paper is to undertake the numerical analysis of the semi-discrete in time weak formulation of (1.1). For the temporal discretization we employ the second order 2-SBDF scheme (1.4), with starting values computed using a first-order scheme (1-SBDF), which leads to a sparse system of linear algebraic equations for each time step. Compared to standard first-order schemes the numerical analysis of the second order scheme (1.4) is more challenging. For ease of exposition we present a priori estimates and an error analysis for the semi-discrete in time weak formulation. The numerical analysis of the corresponding fully-discrete problem requires additional standard techniques from the finite element method for elliptic problems, e.g., interpolation error estimates, inverse estimates, and error estimates for numerical integration [18]. Furthermore, the main challenge in the numerical analysis of the fully-discrete problem is due to the temporal discretization, involving a three level approximation of the time derivative and asymmetry of the approximate reaction kinetics. The methodology in this paper generalizes some techniques applied previously to first-order, two level finite element methods for reaction-diffusion systems [10,28,29] to the three level setting.

In addition to the theoretical aims given above, we present numerical results for a fully-discrete finite element approximation of (1.1) that demonstrate the characteristic Turing patterns of this system. For the spatial discretization we use the standard Galerkin finite element method with piecewise linear continuous basis functions (and 'Lumped Masses', [48]). We also comment on the correct procedure for simulating pattern formation in general reaction-diffusion systems.

In Sect. 2 we initially consider the spatially homogeneous system, followed by the construction of an invariant rectangle in phase space that leads to the global well-posedness of the classical solutions for the full reaction-diffusion system. The semi-discrete in time estimates and optimal error bound are derived in Sect. 3, while the fully-discrete approximations and results of numerical experiments are presented in Sect. 4. Concluding comments are made in Sect. 5 and some auxiliary details placed in an appendix.

2 Mathematical preliminaries

2.1 Function spaces

Standard notation is used for the Sobolev spaces. The usual $L^2(\Omega)$ inner product over Ω with norm $\|\cdot\|_0$ is denoted $(\cdot,\cdot)$, and $L^p(\Omega)$, $1 \le p < \infty$, is the space of pth-integrable functions on Ω, with norm $\|\cdot\|_{0,p}$. Furthermore, we denote $L^p_{\text{loc}}(\Omega)$ by the set $\{f \,:\, f \in L^p(K) \;\text{ for every } K \overset{c}{\hookrightarrow} \Omega\}$, where '$\overset{c}{\hookrightarrow}$' denotes compact injection. Continuous injection is denoted '$\hookrightarrow$'. We let $\langle\cdot,\cdot\rangle$ denote the duality pairing between

$(H^1(\Omega))'$ and $H^1(\Omega)$. The $H^1(\Omega)$ semi-norm will be denoted by $|\cdot|_1$ and the norm of the dual space $(H^1(\Omega))'$ is denoted $\|\cdot\|_*$. A standard Banach space we use is $L^\infty(\Omega)$, with associated essential supremum norm

$$\|u\|_{0,\infty} \equiv \|u\|_{L^\infty(\Omega)} := \inf\{M \,:\, |u(x)| \le M \quad \text{a.e. on } \Omega\}.$$

We also define function spaces depending on space and time (e.g., [57], p. 45). Let X be a Banach space and $p \in [1, \infty]$. Denote $L^p(0, T; X)$ to be the Banach space of all measurable functions $u : (0, T) \mapsto X$ such that $t \mapsto \|u(t)\|_X$ is in $L^p(0, T)$, with norm

$$\|u\|_{L^p(0,T;X)} := \left(\int_0^T \|u(t)\|_X^p dt\right)^{1/p} \qquad \text{for} \quad 1 \le p < \infty, \tag{2.1}$$

$$\|u\|_{L^\infty(0,T;X)} := \operatorname*{ess\,sup}_{t\in(0,T)} \|u(t)\|_X \qquad \text{if} \quad p = \infty. \tag{2.2}$$

In addition, we write $L^p(\Omega_T) \equiv L^p(0, T; L^p(\Omega))$.

We assume the standard Hilbert space setup (e.g., [57], p. 55)

$$V \overset{c}{\hookrightarrow} H \equiv H' \hookrightarrow V', \tag{2.3}$$

where each space is dense in the previous one, and $\equiv$ indicates the explicit identification of elements in H and H'.

We recall the well-posedness of the Coercive Homogeneous Neuman Problem [8, p.225]: let $f \in L^2(\Omega)$ and k be a finite constant, then there exists a unique solution $u \in H^1(\Omega)$ of the problem

$$\int_\Omega (\nabla u \cdot \nabla v + kuv)\, dx = \int_\Omega f v\, dx, \qquad \forall v \in H^1(\Omega). \tag{2.4}$$

Throughout we let C denote a finite positive constant independent of the time step Δt.

2.2 Local analysis

In this section we briefly look at the spatially homogeneous system (1.1) with no diffusion present. This will enable the construction of an invariant rectangle in phase space that provides an elementary proof of the well-posedness of the full reaction-diffusion system.

The local dynamics can be analyzed by considering the nullclines ('zero isoclines') of this system, which are the solution curves for

$$v = F(u) := \frac{(a-u)(1+u+Ku^2)}{\rho u},$$
$$v = G(u) := \frac{\alpha b(1+u+Ku^2)}{\rho u + \alpha(1+u+Ku^2)}, \tag{2.5}$$

corresponding to the first and second equations of (1.1). The intersection of the null-clines leads to the following cubic equation

$$-\alpha K u^3 + (a\alpha K - \rho - \alpha)u^2 + (a\rho + a\alpha - \alpha b\rho - \alpha)u + a\alpha = 0, \tag{2.6}$$

which has either three, or one, positive (real) solution(s), corresponding to the number of stationary points (stable, or unstable). The typical nullclines are illustrated in Fig. 1. A consideration of the signs of the kinetic functions f and g on either side of their respective nullclines F and G, readily leads to the following (arbitrarily large) invariant region in the positive quadrant of phase space:

$$\sum_{A,B} := \left\{(u,v) \in [0,\infty)^2 \ : \ 0 \le u \le A, \quad 0 \le v \le B, \quad A \ge a, \quad B \ge b\right\}. \tag{2.7}$$

The case $\Sigma_{a,b}$ is illustrated in Fig. 1.

2.3 Well-posedness of the reaction-diffusion system

Before proving well-posedness of the equations we need to establish the formal setting and re-state the substrate-inhibition system (1.1) with appropriate initial and boundary data.

Let Ω be a bounded and open subset of $\mathbb{R}^2$, with a boundary $\partial\Omega$ of class C^{2+s}, $s > 0$, i.e., $\partial\Omega$ is a 1 dimensional $C^{2+\nu}$ manifold on which Ω lies locally on one side. The model problem is formulated as follows:

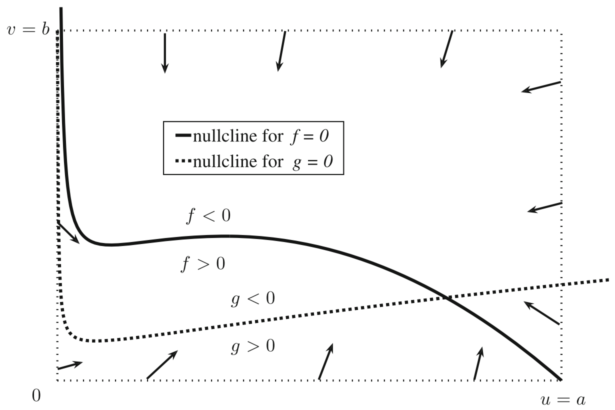

Fig. 1 Typical nullclines for the local kinetics f and g of (1.1) with $a = 50$, $b = 15$, $\rho = 12$, $k = 0.07$, and $\alpha = 1$

Find the functions $u(\mathbf{x}, t)$ and $v(\mathbf{x}, t)$ such that

$$\frac{\partial u}{\partial t} = \Delta u + a - u - h(u, v) \quad \text{in} \quad Q := \Omega \times (0, T), \tag{2.8a}$$

$$\frac{\partial v}{\partial t} = \delta \Delta v + \alpha(b - v) - h(u, v) \quad \text{in} \quad Q, \tag{2.8b}$$

$$h(u, v) := \frac{\rho u v}{1 + u + K u^2}, \tag{2.8c}$$

$$u(\mathbf{x}, 0) = u_0(\mathbf{x}), \qquad v(\mathbf{x}, 0) = v_0(\mathbf{x}), \quad \mathbf{x} \in \Omega \tag{2.8d}$$

$$\frac{\partial u}{\partial \boldsymbol{\nu}} = \frac{\partial v}{\partial \boldsymbol{\nu}} = 0 \quad \text{on} \quad \partial\Omega \times (0, T), \tag{2.8e}$$

where the parameters $a, b, \delta, \alpha, \rho$, and K are real and strictly positive, and $\boldsymbol{\nu}$ denotes the outward normal to $\partial\Omega$. We assume the initial data $u_0(\mathbf{x})$, $v_0(\mathbf{x})$ are in $L^\infty(\Omega) \cap H^1(\Omega)$. It will be convenient to denote the reaction kinetics corresponding to (2.8a) and (2.8b) by $f(u, v)$ and $g(u, v)$ respectively.

Theorem 1 *Let $u_0(\mathbf{x}), v_0(\mathbf{x}) \in L^\infty(\Omega)$. Then there exists a unique classical solution of the substrate-inhibition system* (2.8a)–(2.8e) *for all* $(\mathbf{x}, t) \in \Omega \times [0, \infty)$. *Furthermore, if the initial data is chosen in the invariant region $\sum_{A,B} \subset [0, \infty)^2$ given by* (2.7)*, then* $(u, v) \in \sum_{A,B}$ *for all* $(\mathbf{x}, t) \in \Omega \times [0, \infty)$.

Proof Local existence of solutions is based on well-known semigroup theory (see for example Pazy [50], or Henry [30]). From Proposition 1 in [32] it follows immediately that (2.8a)–(2.8e) has a unique noncontinuable classical solution (u, v) for $(\mathbf{x}, t) \in \Omega \times [0, T_{max})$. To prove global existence of solutions from local existence is straightforward. From Theorem 4.3 of [17] it follows that the invariant region $\sum_{A,B}$ (2.7) is also invariant for the full PDE system. The invariant region yields an L^∞- a priori bound that contradicts non-global existence as solutions either exist for all time, or blow-up in the sup-norm in finite time [9]. □

The substrate-inhibition system (2.8a)–(2.8e) leads to the following weak formulations:

(P) Find $u(\cdot, t), v(\cdot, t) \in H^1(\Omega) \cap L^\infty(\Omega)$ s.t. $\{u(\cdot, 0), v(\cdot, 0)\} = \{u_0(\cdot), v_0(\cdot)\}$ and for almost every $t \in (0, T)$

$$\langle u_t, \eta\rangle + (\nabla u, \nabla \eta) = (a - u - h(u, v)), \eta) \qquad \forall \eta \in H^1(\Omega), \tag{2.9a}$$

$$\langle v_t, \eta\rangle + \delta(\nabla v, \nabla \eta) = (\alpha(b - v) - h(u, v)), \eta) \qquad \forall \eta \in H^1(\Omega), \tag{2.9b}$$

where $h(u, v)$ is defined by (2.8c). The regularity of the classical solutions implies the following strong solution result, which facilitates estimates in later sections.

Corollary 1 *With the assumption that the initial data is in $L^\infty(\Omega) \cap H^1(\Omega)$ the substrate-inhibition system* (2.8a)–(2.8e) *possesses a unique strong solution* $\{u, v\}$ *s.t.*

$$u,\ v \in L^2(0, T; H^2(\Omega)) \cap C([0, T]; H^1(\Omega)), \tag{2.10a}$$

$$\frac{\partial u}{\partial t}, \frac{\partial v}{\partial t} \in L^2(\Omega_T). \tag{2.10b}$$

3 The semi-discrete in time approximations

We provide the analysis of a semi-discrete in time approximation of the problem discussed in the previous section. Discretization in time leads to a sequence of elliptic problems, that can be solved by marching in time from 0 to T.

As the invariant region given by (2.7) is not necessarily invariant for the semi-discrete problem, it is advantageous to modify the reaction kinetics via

$$\frac{\rho u v}{1+u+Ku^2} \longrightarrow \frac{\rho u v}{1+|u|+Ku^2},$$

which avoids the potential singularity of discrete approximations to $h(u, v)$ and also facilitates the derivation of semi-discrete in time a priori estimates in Sect. 3.3. Of course for a correctly converged numerical solution such a modification makes no difference to the solutions. To help simplify the notation in the sequel we define modified reaction kinetics corresponding to (2.8a) and (2.8b) by

$$\widehat{f}(\eta, \chi) := a - \eta - \widehat{h}(\eta, \chi), \quad \widehat{g}(\eta, \chi) := \alpha(b-\chi) - \widehat{h}(\eta, \chi), \tag{3.1a}$$
$$\text{where} \quad \widehat{h}(\eta, \chi) := \rho\eta\chi/(1+|\eta|+K\eta^2). \tag{3.1b}$$

Thus the modified weak formulation can be written as:

($\widehat{\mathbf{P}}$): Find $u(\cdot, t), v(\cdot, t) \in H^1(\Omega) \cap L^\infty(\Omega)$ s.t. $\{u(\cdot, 0), v(\cdot, 0)\} = \{u_0(\cdot), v_0(\cdot)\}$ and for almost every $t \in (0, T)$

$$\langle u_t, \chi\rangle + (\nabla u, \nabla\chi) = (2\widehat{f}(u, v) - \widehat{f}(u, v), \chi) \qquad \forall \chi \in H^1(\Omega), \tag{3.2a}$$
$$\langle v_t, \chi\rangle + \delta(\nabla v, \nabla\chi) = (2\widehat{g}(u, v) - \widehat{g}(u, v), \chi) \qquad \forall \chi \in H^1(\Omega). \tag{3.2b}$$

In later error analysis we need the following local Lipschitz condition on $\widehat{h}$:

Lemma 1 *Let B be a convex subset of $\mathbb{R}^2$. Then*

$$|\widehat{h}(u_1, v_1) - \widehat{h}(u_2, v_2)| \le \rho\big(2 + K|u_1 + u_2|\big)|v_1||u_1 - u_2| + \rho|u_2||v_1 - v_2|$$

for all $(u_1, v_1), (u_2, v_2) \in B$.

Proof The result follows from elementary calculation. □

Lemma 2 *For all $a, b, c \in \mathbb{R}$*

$$(3a - 4b + c)a = \frac{1}{2}[a^2 + (2a-b)^2] - \frac{1}{2}[b^2 + (2b-c)^2] + \frac{1}{2}(a - 2b + c)^2, \tag{3.3a}$$
$$(3a - 4b + c)(a - c) = 2[(a-b)^2 - (b-c)^2] + (a-c)^2. \tag{3.3b}$$

Proof The result follows from elementary calculation. □

This lemma will be used with a, b and c set equal to terms at time levels t_{n+1}, t_n and t_{n-1} respectively.

3.1 Semi-discrete in time weak formulation

Let N be a positive integer and $\Delta t := T/N$ be the fixed time step. Denote the partition of $(0, T)$ by $\sigma_N := \{t_n\}_{n=0}^N$ with $t_n := n\Delta t$. We consider the following semi-discrete in time approximations of Problem (P):

($\mathbf{P}_1^{\Delta t}$) Find $U^1, V^1 \in H^1(\Omega)$ s.t. $\{U^0, V^0\} = \{u(\cdot, 0), v(\cdot, 0)\}$ and $\forall \chi \in H^1(\Omega)$

$$\left(\frac{U^1 - U^0}{\Delta t}, \chi\right) + (\nabla U^1, \nabla \chi) = (\widehat{f}(U^0, V^0), \chi), \tag{3.4a}$$

$$\left(\frac{V^1 - V^0}{\Delta t}, \chi\right) + \delta(\nabla V^1, \nabla \chi) = (\widehat{g}(U^0, V^0), \chi). \tag{3.4b}$$

($\mathbf{P}_2^{\Delta t}$) For $n = 1, \ldots, N-1$ find $U^{n+1}, V^{n+1} \in H^1(\Omega)$ s.t. $\{U^0, V^0\} = \{u(\cdot, 0), v(\cdot, 0)\}$, $\{U^1, V^1\}$ prescribed by ($\mathrm{P}_1^{\Delta t}$) and $\forall \chi \in H^1(\Omega)$

$$\left(\tfrac{3U^{n+1} - 4U^n + U^{n-1}}{2\Delta t}, \chi\right) + (\nabla U^{n+1}, \nabla \chi) = (2\widehat{f}(U^n, V^n) - \widehat{f}(U^{n-1}, V^{n-1}), \chi), \tag{3.5a}$$

$$\left(\tfrac{3V^{n+1} - 4V^n + V^{n-1}}{2\Delta t}, \chi\right) + \delta(\nabla V^{n+1}, \nabla \chi) = (2\widehat{g}(U^n, V^n) - \widehat{g}(U^{n-1}, V^{n-1}), \chi). \tag{3.5b}$$

Note that in practice the time step Δt in ($\mathbf{P}_1^{\Delta t}$) is chosen much smaller than the time steps Δt in ($\mathbf{P}_2^{\Delta t}$). For ease of notation we use the same symbol Δt for both schemes.

3.2 Existence and uniqueness

The existence and uniqueness of the semi-discrete problem is given by the following result:

Theorem 2 *Given $U^0, V^0 \in L^\infty(\Omega)$ and fixed time steps Δt, there exists a unique solution $U^1, V^1 \in H^1(\Omega)$ of the 1st order semi-discrete problem ($\mathbf{P}_1^{\Delta t}$), and a unique solution $\{U^n, V^n\}_{n=2}^N$ of the 2nd order semi-discrete problem ($\mathbf{P}_2^{\Delta t}$), with $U^n, V^n \in H^1(\Omega)$, $n = 2, \ldots, N$.*

Proof To prove existence and uniqueness of the semi-discrete in time weak formulations we recall a result for the Coercive Homogeneous Neumann Problem (see (2.4)) and apply induction. First observe that

$$|\widehat{h}(u, v)| = \left|\frac{\rho u v}{1 + |u| + K u^2}\right| \leq \frac{\rho |u||v|}{|u|} = \rho |v|, \tag{3.6}$$

thus $\widehat{f}(u, v), \widehat{g}(u, v) \in L^2(\Omega)$ if $u, v \in L^2(\Omega)$.

Consider fixed time steps Δt for both the first and second order schemes. Now by assumption U^0, V^0 in $L^\infty(\Omega) \hookrightarrow L^2(\Omega)$. Existence and uniqueness of solutions to the Coercive Homogeneous Neumann Problem (see (2.4)) implies that there exists a unique solution U^1, V^1 of $(\mathbf{P}_1^{\Delta t})$ in $H^1(\Omega) \hookrightarrow L^2(\Omega)$. As $U^0, V^0, U^1, V^1 \in L^2(\Omega)$, existence and uniqueness of solutions to (2.4) yields that there exists a unique solution U^1, V^1 of $(\mathbf{P}_2^{\Delta t})$ in $H^1(\Omega) \hookrightarrow L^2(\Omega)$. Proceeding inductively, we have a unique solution $U^n, V^n \in H^1(\Omega)$, for $n = 2, \ldots, N$. □

We note that this result does not bound the semi-discrete solutions *uniformly* with respect to Δt, which is the purpose of the next section.

3.3 A priori estimates

To derive a semi-discrete error estimate in Sect. 3.4 we prove two a priori estimates bounding U^n and V^n independent of Δt. We first require a lemma uniformly bounding solutions after the first time step.

Lemma 3 *Assume* $U^0, V^0 \in L^\infty(\Omega) \cap H^1(\Omega)$. *Then the solution* $\{U^1, V^1\}$ *of* $(\mathbf{P}_1^{\Delta t})$ *satisfies the following uniform bounds:*

$$\|U^1 - U^0\|_0 + \|V^1 - V^0\|_0 \le C(\Delta t)^{1/2}, \tag{3.7a}$$

$$|U^1 - U^0|_1 + |V^1 - V^0|_1 \le C, \tag{3.7b}$$

$$\|U^1\|_1 + \|V^1\|_1 \le C. \tag{3.7c}$$

Proof The proof of (3.7a) and (3.7b) follows from standard discrete energy techniques applied to scheme $(\mathbf{P}_1^{\Delta t})$ (see e.g. [28,29]). Result (3.7c) follows from the assumptions on the initial data and (3.7a)–(3.7b). □

We also require a bound on the reaction-kinetics in L^2, namely:

Lemma 4

$$\|\widehat{f}(u, v)\|_0^2 \le C(1 + \|u\|_0^2 + \|v\|_0^2), \quad \forall u, v \in L^2(\Omega),$$

$$\|\widehat{g}(u, v)\|_0^2 \le C(1 + \|v\|_0^2), \quad \forall u, v \in L^2(\Omega).$$

Proof The proof is straightforward after noting (3.6). □

We note for future reference a discrete Grönwall lemma [27, Lemma 5.1.1]:

Lemma 5 *Assume* $w_n, \alpha_n, p_n \ge 0$, $0 \le \beta < 1$, *satisfy*

$$w_n + p_n \le \alpha_n + \beta \sum_{k=0}^{n-1} w_{k+1}, \quad \forall n \ge 0,$$

where $\{\alpha_n\}$ *is non-decreasing (with the convention that* $\sum_{k=0}^{-1}(\cdot) = 0$). *Then*

$$w_n + \frac{p_n}{1-\beta} \le \left(\frac{\alpha_n - \beta w_0}{1-\beta}\right) \exp\left(\frac{n\beta}{1-\beta}\right).$$

Theorem 3 *Assume the results and assumptions of Lemma 3 hold, then for sufficiently small Δt the solutions of scheme ($\mathbf{P}_2^{\Delta t}$) satisfy*

$$\max_{1\le n\le N}\{\|U^n\|_1^2+\|V^n\|_1^2\}\le C, \tag{3.8a}$$

$$\max_{1\le n\le N-1}\{\|U^{n+1}-U^n\|_0^2+\|V^{n+1}-V^n\|_0^2\}\le C\Delta t, \tag{3.8b}$$

$$\sum_{n=1}^{N-1}\{\|U^{n+1}-U^n\|_0^2+\|V^{n+1}-V^n\|_0^2\}\le C\Delta t, \tag{3.8c}$$

$$\sum_{n=1}^{N-1}\{|U^{n+1}-U^n|_1^2+|V^{n+1}-V^n|_1^2\}\le C. \tag{3.8d}$$

Proof The semi-discrete a priori bounds are proved via the following two estimates:

3.3.1 Estimate I

In scheme ($\mathbf{P}_2^{\Delta t}$) choose $\chi = U^{n+1}$ in (3.5a), and $\chi = V^{n+1}$ in (3.5b). Applying (3.3a), the Cauchy-Schwarz inequality and Lemma 4 yields

$$\begin{aligned}&\frac{1}{4\Delta t}[\|U^{n+1}\|_0^2+\|2U^{n+1}-U^n\|_0^2]-\frac{1}{4\Delta t}[\|U^n\|_0^2+\|2U^n-U^{n-1}\|_0^2]\\&\quad+\frac{1}{4\Delta t}\|U^{n+1}-2U^n+U^{n-1}\|_0^2+|U^{n+1}|_1^2\\&\le\|U^{n+1}\|_0^2+C(1+\|U^n\|_0^2+\|V^n\|_0^2+\|U^{n-1}\|_0^2+\|V^{n-1}\|_0^2),\end{aligned} \tag{3.9}$$

and

$$\begin{aligned}&\frac{1}{4\Delta t}[\|V^{n+1}\|_0^2+\|2V^{n+1}-V^n\|_0^2]-\frac{1}{4\Delta t}[\|V^n\|_0^2+\|2V^n-V^{n-1}\|_0^2]\\&\quad+\frac{1}{4\Delta t}\|V^{n+1}-2V^n+V^{n-1}\|_0^2+\delta|V^{n+1}|_1^2\\&\le\|V^{n+1}\|_0^2+C(1+\|V^n\|_0^2+\|V^{n-1}\|_0^2).\end{aligned} \tag{3.10}$$

Now add the inequalities (3.9) and (3.10), multiply through by $4\Delta t$, discard terms of the form $(a-2b+c)^2$ and $(2a-b)^2$, change the notation from n to i, and sum over all $i=1,\dots,n-1$ to obtain

$$\begin{aligned}&\|U^n\|_0^2+\|V^n\|_0^2+4\Delta t\sum_{i=1}^{n-1}|U^{i+1}|_1^2+4\delta\Delta t\sum_{i=1}^{n-1}|V^{i+1}|_1^2\\&\le C+C\Delta t\sum_{i=1}^{n-1}(\|U^{i+1}\|_0^2+\|V^{i+1}\|_0^2).\end{aligned} \tag{3.11}$$

Applying the discrete Grönwall Lemma 5 to (3.11) and noting that $C\Delta t < 1$ for Δt sufficiently small yields

$$\|U^n\|_0^2 + \|V^n\|_0^2 + \left(\frac{4\Delta t}{1 - C\Delta t}\right)\sum_{i=1}^{n-1}(|U^{i+1}|_1^2 + \delta|V^{i+1}|_1^2) \leq \left(\frac{C}{1 - C\Delta t}\right)\exp\left(\frac{Ct_n}{1 - C\Delta t}\right) \quad (t_n := n\Delta t), \tag{3.12}$$

after recalling the assumptions on the initial data. This leads to the following uniform bound for the solutions of $(\mathbf{P}_2^{\Delta t})$:

$$\max_{1\leq n\leq N}\{\|U^n\|_0 + \|V^n\|_0\} \leq C. \tag{3.13}$$

3.3.2 Estimate II

In scheme $(\mathbf{P}_2^{\Delta t})$ choose $\chi = (U^{n+1} - U^{n-1})/\Delta t$ in (3.5a), and $\chi = (V^{n+1} - V^{n-1})/\Delta t$ in (3.5b). Adding the resulting equations and applying the identity (3.3b) yields

$$\begin{aligned}
&\frac{1}{(\Delta t)^2}\big[(\|U^{n+1} - U^n\|_0^2 + \|V^{n+1} - V^n\|_0^2) - (\|U^n - U^{n-1}\|_0^2 + \|V^n - V^{n-1}\|_0^2)\big]\\
&\quad+\frac{1}{2(\Delta t)^2}\big[\|U^{n+1} - U^{n-1}\|_0^2 + \|V^{n+1} - V^{n-1}\|_0^2\big] + \frac{1}{2\Delta t}\big[|U^{n+1} - U^{n-1}|_1^2\\
&\quad+\delta|V^{n+1} - V^{n-1}|_1^2\big] + \frac{1}{2\Delta t}\big[|U^{n+1}|_1^2 - |U^{n-1}|_1^2\big] + \frac{\delta}{2\Delta t}\big[|V^{n+1}|_1^2 - |V^{n-1}|_1^2\big]\\
&= 2\left(\widehat{f}(U^n, V^n), \tfrac{U^{n+1}-U^{n-1}}{\Delta t}\right) + 2\left(\widehat{g}(U^n, V^n), \tfrac{V^{n+1}-V^{n-1}}{\Delta t}\right)\\
&\quad-\left(\widehat{f}(U^{n-1}, V^{n-1}), \tfrac{U^{n+1}-U^{n-1}}{\Delta t}\right) - \left(\widehat{g}(U^{n-1}, V^{n-1}), \tfrac{V^{n+1}-V^{n-1}}{\Delta t}\right).
\end{aligned}\tag{3.14}$$

Application of Young's inequality and using Lemma 4 bounds the right hand side of (3.14) via

$$\begin{aligned}
&8\|\widehat{f}(U^n, V^n)\|_0^2 + 8\|\widehat{g}(U^n, V^n)\|_0^2 + 2\|\widehat{f}(U^{n-1}, V^{n-1})\|_0^2 + 2\|\widehat{g}(U^{n-1}, V^{n-1})\|_0^2\\
&\quad+\frac{1}{4}\left\|\tfrac{U^{n+1}-U^{n-1}}{\Delta t}\right\|_0^2 + \frac{1}{4}\left\|\tfrac{V^{n+1}-V^{n-1}}{\Delta t}\right\|_0^2\\
&\leq C + C\big[\|U^n\|_0^2 + \|V^n\|_0^2 + \|U^{n-1}\|_0^2 + \|V^{n-1}\|_0^2\big]\\
&\quad+\frac{1}{4}\left\|\tfrac{U^{n+1}-U^{n-1}}{\Delta t}\right\|_0^2 + \frac{1}{4}\left\|\tfrac{V^{n+1}-V^{n-1}}{\Delta t}\right\|_0^2.
\end{aligned}\tag{3.15}$$

It follows from (3.14) and (3.15), kick-back of the last two terms in (3.15), and the uniform bound (3.13) that

$$
\frac{1}{(\Delta t)^2}\big[(\|U^{n+1}-U^n\|_0^2+\|V^{n+1}-V^n\|_0^2)-(\|U^n-U^{n-1}\|_0^2+\|V^n-V^{n-1}\|_0^2)\big]
+\frac{1}{4}\left\|\frac{U^{n+1}-U^{n-1}}{\Delta t}\right\|_0^2+\frac{1}{4}\left\|\frac{V^{n+1}-V^{n-1}}{\Delta t}\right\|_0^2+\frac{1}{2\Delta t}\big[|U^{n+1}-U^{n-1}|_1^2
+\delta|V^{n+1}-V^{n-1}|_1^2\big]+\frac{1}{2\Delta t}\big[|U^{n+1}|_1^2-|U^{n-1}|_1^2\big]+\frac{\delta}{2\Delta t}\big[|V^{n+1}|_1^2-|V^{n-1}|_1^2\big]
\le C+C\big[\|U^n\|_0^2+\|V^n\|_0^2+\|U^{n-1}\|_0^2+\|V^{n-1}\|_0^2\big]\le C.
$$

After a change of notation from n to i, summing over all $i=1,\ldots,n-1$, noting the telescopic sum property $\sum_{i=1}^{n-1}(a_{i+1}-a_{i-1})=(a_n+a_{n-1})-(a_1+a_0)$, taking terms at t_0 and t_1 to the right hand side, multiplying through by $(\Delta t)^2$, and recalling Lemma 3 yields:

$$
\|U^n-U^{n-1}\|_0^2+\|V^n-V^{n-1}\|_0^2+\frac{1}{4}\sum_{i=1}^{n-1}\big\{\|U^{i+1}-U^{i-1}\|_0^2+\|V^{i+1}-V^{i-1}\|_0^2\big\}
+\frac{\Delta t}{2}\sum_{i=1}^{n-1}\big\{|U^{i+1}-U^{i-1}|_1^2+\delta|V^{i+1}-V^{i-1}|_1^2\big\}+\frac{\Delta t}{2}(|U^n|_1^2+|U^{n-1}|_1^2)
+\delta\Delta t(|V^n|_1^2+|V^{n-1}|_1^2)\le C\Delta t.
$$

Thus after noting Lemma 3 and (3.13) the results of Theorem 3 follow. □

3.4 Error bound

Let $\varepsilon_u^{n+1},\varepsilon_v^{n+1}\in(H^1(\Omega))'$ denote the local truncation errors (see, e.g. [52,53]) at time-step t_{n+1} such that for all $\chi\in H^1(\Omega)$:

$$
\begin{aligned}
\langle\varepsilon_u^{n+1},\chi\rangle &:= \frac{1}{2\Delta t}\langle 3u(t_{n+1})-4u(t_n)+u(t_{n-1}),\chi\rangle+(\nabla u(t_{n+1}),\nabla\chi)\\
&\quad-\langle 2\widehat{f}(u(t_n),v(t_n))-\widehat{f}(u(t_{n-1}),v(t_{n-1})),\chi\rangle,\\
\langle\varepsilon_v^{n+1},\chi\rangle &:= \frac{1}{2\Delta t}\langle 3v(t_{n+1})-4v(t_n+v(t_{n-1})),\chi\rangle+\delta\,(\nabla v(t_{n+1}),\nabla\chi)\\
&\quad-\langle 2\widehat{g}(u(t_n),v(t_n))-\widehat{g}(u(t_{n-1}),v(t_{n-1})),\chi\rangle.
\end{aligned}\tag{3.16}
$$

The pointwise errors $e_u^n, e_v^n\in H^1(\Omega)$ are defined by

$$
e_u^n=u(t_n)-U^n,\qquad e_v^n=v(t_n)-V^n,\qquad \text{for } 0\le n\le N.\tag{3.17}
$$

Lemma 6 *Assume the classical solution of* (1.1) *has the following regularity:*

$$
\frac{d^2u}{dt^2},\frac{d^2v}{dt^2}\in L^2(0,T,H^1(\Omega)),\quad \frac{d^3u}{dt^3},\frac{d^3v}{dt^3}\in L^2(0,T,(H^1(\Omega))').
$$

Then the truncation error satisfies the following bound:

$$\left(\Delta t \sum_{n=1}^{N} \left(\|\varepsilon_u^n\|_*^2 + \|\varepsilon_v^n\|_*^2\right)\right)^{\frac{1}{2}}$$
$$\leq C(\Delta t)^2 \left[\int_0^T \left(\left\|\frac{d^2u}{dt^2}(t)\right\|_*^2 + \left\|\frac{d^2v}{dt^2}(t)\right\|_*^2 + \left\|\frac{d^3u}{dt^3}(t)\right\|_*^2 + \left\|\frac{d^3v}{dt^3}(t)\right\|_*^2\right) dt\right]^{\frac{1}{2}}. \tag{3.18}$$

Proof First we expand $u(t_{n-1})$, $v(t_{n-1})$ and $u(t_n)$, $v(t_n)$ about t_{n+1} by Taylor's formula to second order with integral remainder, to obtain

$$\frac{3u(t_{n+1}) - 4u(t_n) + u(t_{n-1})}{2\Delta t} = \frac{du}{dt}(t_{n+1}) + \Delta t \int_{t_{n-1}}^{t_{n+1}} K_1(t) \frac{d^3u}{dt^3}(t) dt,$$
$$\frac{3v(t_{n+1}) - 4v(t_n) + v(t_{n-1})}{2\Delta t} = \frac{dv}{dt}(t_{n+1}) + \Delta t \int_{t_{n-1}}^{t_{n+1}} K_1(t) \frac{d^3v}{dt^3}(t) dt,$$

where $K_1(t)$ is bounded by a constant independent of Δt, u and v. Using the Taylor expansion to first order, relation (3.1a), and recalling that $\widehat{f} \equiv f, \widehat{g} \equiv g$ on $\mathbb{R}_+^2$, we have

$$\begin{aligned}
&2\widehat{f}(u(t_n), v(t_n)) - \widehat{f}(u(t_{n-1}), v(t_{n-1}))\\
&\quad = a - u(t_{n+1}) + (\Delta t)^2 \int_{t_{n-1}}^{t_{n+1}} K_2(t) \frac{d^2u}{dt^2}(t) dt - 2\widehat{h}(u(t_n), v(t_n))\\
&\qquad + \widehat{h}(u(t_{n-1}), v(t_{n-1})), 2\widehat{g}(u(t_n), v(t_n)) - \widehat{g}(u(t_{n-1}), v(t_{n-1}))\\
&\quad = \alpha b - \alpha v(t_{n+1}) + \alpha(\Delta t)^2 \int_{t_{n-1}}^{t_{n+1}} K_2(t) \frac{d^2v}{dt^2}(t) dt - 2\alpha\widehat{h}(u(t_n), v(t_n))\\
&\qquad + \widehat{h}(u(t_{n-1}), v(t_{n-1})),
\end{aligned}$$

where $K_2(t)$ is also bounded by a constant independent of u, v and Δt. Substituting these expansions into (3.16) and using the fact that $u, v > 0$ we find that

$$\begin{aligned}
\langle \varepsilon_u^{n+1}, \chi \rangle &= \left\langle \frac{du}{dt}(t_{n+1}), \chi \right\rangle + (\nabla u(t_{n+1}), \nabla \chi)\\
&\quad + \left(\Delta t \int_{t_{n-1}}^{t_{n+1}} K_1(t) \frac{d^3u}{dt^3}(t) dt - a + u(t_{n+1}), \chi\right)
\end{aligned}$$

$$-\left((\Delta t)^2\int_{t_{n-1}}^{t_{n+1}}K_2(t)\frac{d^2u}{dt^2}(t)dt+2h(u(t_n),v(t_n))-h(u(t_{n-1}),v(t_{n-1})),\chi\right),$$

$$\langle\varepsilon_v^{n+1},\chi\rangle=\left\langle\frac{dv}{dt}(t_{n+1}),\chi\right\rangle+\delta(\nabla v(t_{n+1}),\nabla\chi)$$
$$+\left(\Delta t\int_{t_{n-1}}^{t_{n+1}}K_1(t)\frac{d^3v}{dt^3}(t)dt-\alpha b+\alpha v(t_{n+1}),\chi\right)$$
$$-\left(\alpha(\Delta t)^2\int_{t_{n-1}}^{t_{n+1}}K_2(t)\frac{d^2v}{dt^2}(t)dt+2h(u(t_n),v(t_n))-h(u(t_{n-1}),v(t_{n-1})),\chi\right).$$

Using (2.8a), (2.8b) at t_{n+1}, we obtain

$$\langle\varepsilon_u^{n+1},\chi\rangle=\langle-h(u(t_{n+1}),v(t_{n+1}))+2h(u(t_n),v(t_n))-h(u(t_{n-1}),v(t_{n-1})),\chi\rangle$$
$$+\left(\Delta t\int_{t_{n-1}}^{t_{n+1}}K_1(t)\frac{d^3u}{dt^3}(t)dt-(\Delta t)^2\int_{t_{n-1}}^{t_{n+1}}K_2(t)\frac{d^2u}{dt^2}(t)dt,\chi\right),$$
$$\langle\varepsilon_v^{n+1},\chi\rangle=\langle-h(u(t_{n+1}),v(t_{n+1}))+2h(u(t_n),v(t_n))-h(u(t_{n-1}),v(t_{n-1})),\chi\rangle$$
$$+\left(\Delta t\int_{t_{n-1}}^{t_{n+1}}K_1(t)\frac{d^3v}{dt^3}(t)dt-(\Delta t)^2\int_{t_{n-1}}^{t_{n+1}}K_2(t)\frac{d^2v}{dt^2}(t)dt,\chi\right).\quad(3.19)$$

By Taylor's theorem in two variables (see e.g., [5]), we have

$$-h(u(t_{n+1}),v(t_{n+1}))+2h(u(t_n),v(t_n))-h(u(t_{n-1}),v(t_{n-1}))$$
$$=\frac{\partial h}{\partial u}(u(t_{n+1}),v(t_{n+1}))(\Delta t)^2\int_{t_{n-1}}^{t_{n+1}}K_2(t)\frac{d^2u}{dt^2}dt$$
$$+\frac{\partial h}{\partial v}(u(t_{n+1}),v(t_{n+1}))(\Delta t)^2\int_{t_{n-1}}^{t_{n+1}}K_2(t)\frac{d^2v}{dt^2}dt+R_1^n-R_1^{n-1},$$

with $\|R_1^n-R_1^{n-1}\|_*\le C(\Delta t)^3$. Then by (2.8c) this gives

$$|\langle-h(u(t_{n+1}),v(t_{n+1}))+2h(u(t_n),v(t_n))-h(u(t_{n-1}),v(t_{n-1})),\chi\rangle|$$
$$\le C_3(\Delta t)^2\int_{t_{n-1}}^{t_{n+1}}\left(\left\|\frac{d^2u}{dt^2}(t)\right\|_*+\left\|\frac{d^2v}{dt^2}(t)\right\|_*\right)dt\|\chi\|_1,\quad(3.20)$$

where the constant $C_3 = C_3(\|v\|_{C([0,T],H^1(\Omega))})$ is independent of n and Δt. Therefore (3.19) and (3.20) imply

$$\|\varepsilon_u^{n+1}\|_* \leq C_3(\Delta t)^2 + c_1\Delta t \int_{t_{n-1}}^{t_{n+1}} \left\|\frac{d^3u}{dt^3}(t)\right\|_* dt + c_2(\Delta t)^2 \int_{t_{n-1}}^{t_{n+1}} \left\|\frac{d^2u}{dt^2}(t)\right\|_* dt,$$

$$\|\varepsilon_v^{n+1}\|_* \leq C_3(\Delta t)^2 + c_1\Delta t \int_{t_{n-1}}^{t_{n+1}} \left\|\frac{d^3v}{dt^3}(t)\right\|_* dt + c_2(\Delta t)^2 \int_{t_{n-1}}^{t_{n+1}} \left\|\frac{d^2v}{dt^2}(t)\right\|_* dt.$$

Finally

$$\|\varepsilon_u^{n+1}\|_*^2 \leq C(\Delta t)^3 \left(\int_{t_{n-1}}^{t_{n+1}} \left(\left\|\frac{d^3u}{dt^3}(t)\right\|_*^2 + \left\|\frac{d^2u}{dt^2}(t)\right\|_*^2 \right) dt \right),$$

$$\|\varepsilon_v^{n+1}\|_*^2 \leq C(\Delta t)^3 \left(\int_{t_{n-1}}^{t_{n+1}} \left(\left\|\frac{d^3v}{dt^3}(t)\right\|_*^2 + \left\|\frac{d^2v}{dt^2}(t)\right\|_*^2 \right) dt \right),$$

which yields (3.18). □

To establish the error estimate we first prove a stability property.

Lemma 7 *For Δt sufficiently small, the $(\mathbf{P}_2^{\Delta t})$ scheme satisfies the following stability property*

$$\|e_u^n\|_0^2 + \|e_v^n\|_0^2 + \left(\frac{2\Delta t}{1-C\Delta t}\right) \sum_{k=2}^{n} \left(|e_u^k|_1^2 + \delta|e_v^k|_1^2\right) \leq \left(\frac{1}{1-C\Delta t}\right)$$
$$\times \left[5\|e_u^1\|_0^2 + 5\|e_v^1\|_0^2 + 4\Delta t \sum_{k=2}^{n} \left(\|\varepsilon_u^k\|_*^2 + \frac{1}{\delta}\|\varepsilon_v^k\|_*^2\right)\right] \exp\left(\frac{Ct_n}{1-C\Delta t}\right).$$

Proof Subtract (3.5a)–(3.5b) from (3.16) to obtain

$$\begin{aligned}
&\frac{1}{2\Delta t}\langle 3e_u^{n+1} - 4e_u^n + e_u^{n-1}, \chi\rangle + \left(\nabla e_u^{n+1}, \nabla\chi\right) \\
&\quad = \langle \varepsilon_u^{n+1}, \chi\rangle + \langle 2\widehat{f}(u(t_n), v(t_n)) - \widehat{f}(u(t_{n-1}), v(t_{n-1})) \\
&\qquad -2\widehat{f}(U^n, V^n) + \widehat{f}(U^{n-1}, V^{n-1}), \chi\rangle, \\
&\frac{1}{2\Delta t}\langle 3e_v^{n+1} - 4e_v^n + e_v^{n-1}, \chi\rangle + \delta\left(\nabla e_v^{n+1}, \nabla\chi\right) \\
&\quad = \langle \varepsilon_v^{n+1}, \chi\rangle + \langle 2\widehat{g}(u(t_n), v(t_n)) - \widehat{g}(u(t_{n-1}), v(t_{n-1})) \\
&\qquad -2\widehat{g}(U^n, V^n) + \widehat{g}(U^{n-1}, V^{n-1}), \chi\rangle.
\end{aligned} \tag{3.21}$$

Then take $\chi = e_u^{n+1}$ in the first equation, $\chi = e_v^{n+1}$ in the second, and use (3.1a) to obtain

$$
\begin{aligned}
&\frac{1}{2\Delta t}\langle 3e_u^{n+1} - 4e_u^n + e_u^{n-1}, e_u^{n+1}\rangle + \|\nabla e_u^{n+1}\|^2 \\
&\quad = \langle \varepsilon_u^{n+1}, e_u^{n+1}\rangle + \langle\, 2\widehat{f}(u(t_n), v(t_n)) - 2\widehat{f}(U^n, V^n) \\
&\qquad - \widehat{f}(u(t_{n-1}), v(t_{n-1})) + \widehat{f}(U^{n-1}, V^{n-1}), e_u^{n+1}\rangle \\
&\quad = \langle \varepsilon_u^{n+1}, e_u^{n+1}\rangle - 2\langle e_u^n + \big(\widehat{h}(u(t_n), u(t_n) - \widehat{h}(U^n, V^n)\big), e_u^{n+1}\rangle \\
&\qquad + \langle e_u^{n-1} + \big(\widehat{h}(u(t_{n-1}), u(t_{n-1}) - \widehat{h}(U^{n-1}, V^{n-1})\big), e_u^{n+1}\rangle, \\
&\frac{1}{2\Delta t}\langle 3e_v^{n+1} - 4e_v^n + e_v^{n-1}, e_v^{n+1}\rangle + \delta\|\nabla e_v^{n+1}\|^2 \\
&\quad = \langle \varepsilon_v^{n+1}, e_v^{n+1}\rangle + 2\langle \widehat{g}(u(t_n), v(t_n)) - \widehat{g}(U^n, V^n) \\
&\qquad - \widehat{g}(u(t_{n-1}), v(t_{n-1})) - \widehat{g}(U^{n-1}, V^{n-1}), e_v^{n+1}\rangle \\
&\quad = \langle \varepsilon_v^{n+1}, e_v^{n+1}\rangle + 2\langle -\alpha e_v^n - \widehat{h}(u(t_n), v(t_n)) + \widehat{h}(U^n, V^n), e_v^{n+1}\rangle \\
&\qquad + \langle \alpha e_v^{n-1} + \widehat{h}(u(t_{n-1}), v(t_{n-1})) - \widehat{h}(U^{n-1}, V^{n-1}), e_v^{n+1}\rangle.
\end{aligned}
$$

By use of Lemma 1 we have

$$
\begin{aligned}
&\widehat{f}(u(t_n), v(t_n)) - \widehat{f}(U^n, V^n) \\
&\quad = -e_u^n - \Big(\widehat{h}(u(t_n), v(t_n)) - \widehat{h}(U^n, V^n)\Big) \\
&\quad \le |e_u^n|\Big[1 + \rho(2 + K|u(t_n) + U^n|)|v(t_n)|\Big] + \rho|e_v^n||U^n|, \\
&\widehat{g}(u(t_n), v(t_n)) - \widehat{g}(U^n, V^n) \\
&\quad = -\alpha e_v^n - \Big(\widehat{h}(u(t_n), v(t_n)) - \widehat{h}(U^n, V^n)\Big) \\
&\quad \le |e_v^n|(\alpha + |U^n|) + |e_u^n|\Big[1 + \rho(2 + K|u(t_n) + U^n|)|v(t_n)|\Big].
\end{aligned}
$$

This yields

$$
\begin{aligned}
&\frac{1}{2\Delta t}\langle 3e_u^{n+1} - 4e_u^n + e_u^{n-1}, e_u^{n+1}\rangle + \|\nabla e_u^{n+1}\|^2 \le \langle \varepsilon_u^{n+1}, e_u^{n+1}\rangle \\
&\quad + 2\int_\Omega |e_u^{n+1}|\left\{|e_u^n|[1 + \rho(2 + K|u(t_n) + U^n|)|v(t_n)|] + \rho|e_v^n||U^n|\right\} dx \\
&\quad + \int_\Omega |e_u^{n+1}|\Big\{|e_u^{n-1}|[1+\rho(2+K|u(t_{n-1})+U^{n-1}|)|v(t_{n-1})|]+\rho|e_v^{n-1}||U^{n-1}|\Big\}\, dx,
\end{aligned}
$$

$$\frac{1}{2\Delta t}\langle 3e_v^{n+1} - 4e_v^n + e_v^{n-1}, e_v^{n+1}\rangle + \delta\|\nabla e_v^{n+1}\|^2 \le \langle \varepsilon_v^{n+1}, e_v^{n+1}\rangle$$
$$+ \int_\Omega |e_v^{n+1}|\Big\{2|e_v^n|(\alpha + \rho|U^n|) + 2|e_u^n|[1 + \rho(2 + K|u(t_n) + U^n|)|v(t_n)|]$$
$$+ |e_v^{n-1}|(\alpha + \rho|U^{n-1}|) + |e_u^{n-1}|[1 + \rho(2 + K|u(t_{n-1}) + U^{n-1}|)|v(t_{n-1})|]\Big\}dx.$$

Add the two relations, use Young's inequality, the uniform bound (3.8a), the definition of the $H^1(\Omega)$ norm and the Sobolev embedding result to obtain

$$\frac{1}{2\Delta t}\langle 3e_u^{n+1} - 4e_u^n + e_u^{n-1}, e_u^{n+1}\rangle + \frac{1}{2\Delta t}\langle 3e_v^{n+1} - 4e_v^n + e_v^{n-1}, e_v^{n+1}\rangle + \|\nabla e_u^{n+1}\|^2$$
$$+ \delta\|\nabla e_v^{n+1}\|^2 \le \|\varepsilon_u^{n+1}\|_*^2 + \frac{1}{\delta}\|\varepsilon_v^{n+1}\|_*^2 + \frac{1}{2}\|\nabla e_u^{n+1}\|_0^2 + \frac{\delta}{2}\|\nabla e_v^{n+1}\|_0^2$$
$$+ \frac{1}{2}\|e_u^{n+1}\|_0^2 + \frac{\delta}{2}\|e_v^{n+1}\|_0^2 + C\Big(\|e_u^n\|_0^2 + \|e_v^n\|_0^2 + \|e_u^{n-1}\|_0^2 + \|e_v^{n-1}\|_0^2\Big).$$

After kick-back and multiplying by 2 we obtain

$$\frac{1}{\Delta t}\langle 3e_u^{n+1} - 4e_u^n + e_u^{n-1}, e_u^{n+1}\rangle + \frac{1}{\Delta t}\langle 3e_v^{n+1} - 4e_v^n + e_v^{n-1}, e_v^{n+1}\rangle + \|\nabla e_u^{n+1}\|_0^2$$
$$+ \delta\|\nabla e_v^{n+1}\|_0^2 \le 2\|\varepsilon_u^{n+1}\|_*^2 + \frac{2}{\delta}\|\varepsilon_v^{n+1}\|_*^2 + \|e_u^{n+1}\|_0^2 + \delta\|e_v^{n+1}\|_0^2$$
$$+ C\Big(\|e_u^n\|_0^2 + \|e_v^n\|_0^2 + \|e_u^{n-1}\|_0^2 + \|e_v^{n-1}\|_0^2\Big).$$

Changing notation from n to k, summing k from 1 to $n-1$, using Lemma 2, applying a telescopic sum property, noting that $e_u^0 = e_v^0 = 0$, and multiplying by $2\Delta t$ yields

$$\|e_u^n\|_0^2 + \|e_v^n\|_0^2 + 2\Delta t\sum_{k=2}^{n}\Big(\|\nabla e_u^k\|_0^2 + \delta\|\nabla e_v^k\|_0^2\Big) \le 5\|e_u^1\|_0^2 + 5\|e_v^1\|_0^2$$
$$+ 4\Delta t\sum_{k=2}^{n}\Big(\|\varepsilon_u^k\|_*^2 + \frac{1}{\delta}\|\varepsilon_v^k\|_*^2\Big) + C\Delta t\sum_{n=0}^{n-1}\Big(\|e_u^{k+1}\|_0^2 + \|e_v^{k+1}\|_0^2\Big).$$

Application of the discrete Grönwall Lemma 5 concludes the proof. □

Combining Lemmata 6 and 7, and noting the assumption that e_u^1 and e_v^1 are of order $(\Delta t)^2$, leads to the convergence and error estimate of the solution U^n, V^n of $(\mathbf{P}_2^{\Delta t})$.

Theorem 4 *Under the assumptions of Lemma 6, there exists a constant $C(u, v) > 0$ such that*

$$\max_{0\le n\le N}\left(\|u(t_n)-U^n\|_0+\|v(t_n)-V^n\|_0\right)$$
$$+\left(\Delta t\sum_{n=0}^{N}\left(\|\nabla(u(t_n)-U^n)\|_0^2+\delta\|\nabla(v(t_n)-V^n)\|_0^2\right)\right)^{\frac{1}{2}}$$
$$\le C(u,v)\Big(\|u(t_1)-U^1\|_0+\|v(t_1)-V^1\|_0+\|2(u(t_1)-U^1)-(u(t_0)-U^0)\|_0^2$$
$$+\|2(v(t_1)-V^1)-(v(t_0)-V^0)\|_0^2+(\Delta t)^2\Big).$$

4 A fully discrete approximation

Before stating the fully discrete finite element approximations of the Thomas system we recall some standard definitions.

Let $\mathcal{T}^h$ be a quasi-uniform partitioning [18, p. 132] of Ω into disjoint open simplices $\{\tau\}$ with $h_\tau := \operatorname{diam}\tau$ and $h := \max_{\tau\in\mathcal{T}^h} h_\tau$, so that $\overline{\Omega} = \cup_{\tau\in\mathcal{T}^h}\ \overline{\tau}$. We use the standard Galerkin finite element space of piecewise linear continuous functions defined by:

$$S^h := \{v\in C(\overline{\Omega})\ :\ v|_\tau \quad \text{is linear}\ \forall\tau\in\mathcal{T}^h\}\subset H^1(\Omega).$$

We shall also need the Lagrange interpolation operator $\pi^h : C(\overline{\Omega})\mapsto S^h$ s.t. $\pi^h v(x_j) = v(x_j)$ for all $j=0,\dots J$ for nodes $\{x_j\}_{j=0}^J$ of the triangulation. Let $\{\varphi_j\}_{j=0}^J$ be the standard basis for S^h, satisfying $\varphi_j(x_i)=\delta_{ij}$, where $\{x_i\}_{i=0}^J$ is the set of nodes of $\mathcal{T}^h$. A discrete L^2 inner product on $C(\overline{\Omega})$ is then defined by

$$(u,v)^h := \int_\Omega \pi^h(u(x)v(x))\,dx \equiv \sum_{j=0}^{J}\widehat{M}_{jj}u(x_j)v(x_j), \tag{4.1}$$

where $\widehat{M}_{jj} := (1,\varphi_j)\equiv(\varphi_j,\varphi_j)^h>0$, corresponding to the (diagonal) lumped mass matrix $\widehat{M}$.

We study the fully discrete approximation of scheme $(\mathbf{P}_1^{\Delta t})$ for the first time step, and the fully discrete approximation scheme of $(\mathbf{P}_2^{\Delta t})$:

$(\mathbf{P}_1^{h,\Delta t})$ Find $U_h^1, V_h^1\in S^h$ with initial data $\{U_h^0,V_h^0\}=\{\pi^h u_0(x),\pi^h v_0(x)\}$ s.t. for all $\chi_h\in S^h$ we have

$$\frac{1}{\Delta t}\left(U_h^1-U_h^0,\chi_h\right)^h+\left(\nabla U_h^1,\nabla\chi_h\right)=\left(\widehat{f}(U_h^0,V_h^0),\chi_h\right)^h, \tag{4.2a}$$
$$\frac{1}{\Delta t}\left(V_h^1-V_h^0,\chi_h\right)^h+\delta\left(\nabla V_h^1,\nabla\chi_h\right)=\left(\widehat{g}(U_h^0,V_h^0),\chi_h\right)^h. \tag{4.2b}$$

$(\mathbf{P}_2^{h,\Delta t})$ For $n=2,\dots,N$ find $U_h^n, V_h^n\in S^h$ with initial data $\{U_h^0,V_h^0\} = \{\pi^h u_0(x),\pi^h v_0(x)\}$, $\{U_h^1,V_h^1\}$ prescribed by $(\mathrm{P}_1^{h,\Delta t})$, s.t. for all $\chi_h\in S^h$ we have

$$\frac{1}{2\Delta t}\left(3U_h^{n+1}-4U_h^n+U_h^{n-1},\chi_h\right)^h+\left(\nabla U_h^{n+1},\nabla\chi_h\right)$$
$$=\left(2\widehat{f}(U_h^n,V_h^n)-\widehat{f}(U_h^{n-1},V_h^{n-1}),\chi_h\right)^h, \tag{4.3a}$$
$$\frac{1}{2\Delta t}\left(3V_h^{n+1}-4V_h^n+V_h^{n-1},\chi_h\right)^h+\delta\left(\nabla V_h^{n+1},\nabla\chi_h\right)$$
$$=\left(2\widehat{g}(U_h^n,V_h^n)-\widehat{g}(U_h^{n-1},V_h^{n-1}),\chi_h\right)^h. \tag{4.3b}$$

Choosing $U_h^n = \sum_{j=0}^h U_j^n\varphi_j$, $V_h^n = \sum_{j=0}^h V_h^n\varphi_j$, $\chi_h = \varphi_i$, $i = 0,\ldots,T$ in ($\mathbf{P}_2^{h,\Delta t}$), where $U_j^n \approx u(x_j, n\Delta t)$, $V_j^n \approx v(x_j, n\Delta t)$, leads to a sparse linear system with the following block matrix form of $2J+2$ linear equations:

$$\begin{pmatrix} M_1 & O\\ O & M_2\end{pmatrix}\begin{pmatrix}\mathbf{U}^{n+1}\\ \mathbf{V}^{n+1}\end{pmatrix}=\begin{pmatrix}\Lambda(\mathbf{U}^{n-1},\mathbf{V}^{n-1},\mathbf{U}^n,\mathbf{V}^n)\\ \Xi(\mathbf{U}^{n-1},\mathbf{V}^{n-1},\mathbf{U}^n,\mathbf{V}^n)\end{pmatrix},$$

where $\{\mathbf{U}^n\}_i = U_i^n$, $\{\mathbf{V}^n\}_i = V_i^n$. M_1 and M_2 are strictly diagonally dominant and do not change from one time level to the next. Furthermore, because of the block structure of the linear system, we solved the approximate solutions for u and v independently at each time step using the Generalized Minimal Residual Method (GMRES) in MATLAB, preconditioned by incomplete LU factorization.

4.1 Numerical experiments

4.1.1 Simulation of prepattern formation

We repeat a numerical experiment of Murray [44] who used the Thomas system for illustrative purposes to simulate pattern formation over a schematic mammal skin with fixed geometry and various domain sizes. We provide sufficient details of the numerical procedure so that results can be verified in future work, using the numerical schemes presented in this paper, or using other numerical methods.

Schemes ($\mathbf{P}_1^{h,\Delta t}$) with ($\mathbf{P}_2^{h,\Delta t}$) were solved over $\Omega\times(0,T]$, where Ω is a schematic mammal skin domain fitting in the rectangles $[0,L_x]\times[0,L_y]$, with $L_x := 512/2^{(i-1)}$ and $Ly := 768/2^{(i-1)}$, $i = 3, 5, 7, 9, 11$ (Fig. 2). Homogeneous Neumann boundary conditions were employed with initial data (u_0, v_0) prescribed as perturbations of the stationary states (u_c, v_c) of the corresponding spatially homogeneous system on every point of the computational domain. The stationary states (u_c, v_c) were perturbed using a truncated double Fourier series

$$p(x,y) := \sum_{s=1}^{20}\left\{\sum_{r=1}^{20} z_{rs}\sin\left(\frac{s\pi x}{L_x}\right)\cos\left(\frac{r\pi y}{L_y}\right)\right\}, \tag{4.4}$$

scaled to be on $[-1, 1]$, denoted $\widehat{p}(x, y)$, with coefficients z_{rs} drawn from a simple pseudo random number generator `D_UNIFORM_01` [37] (see Appendix for more details). In particular, we prescribed

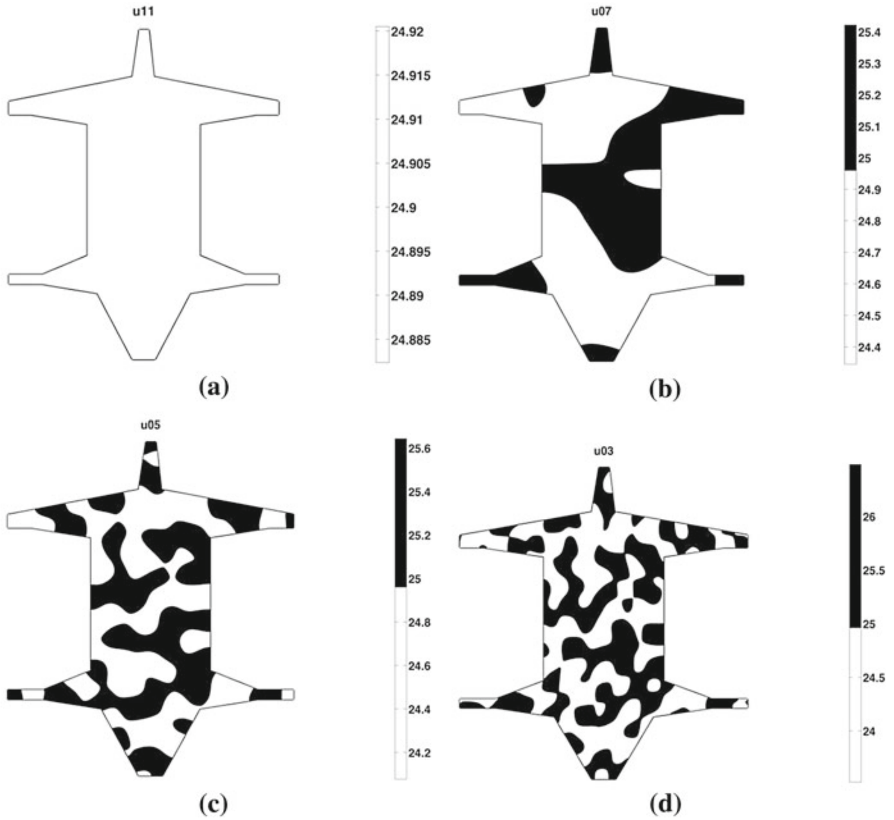

Fig. 2 Approximate solutions U^n for scheme $(\mathbf{P}_2^{\Delta t})$ at time $T = 500$. We used an unstructured mesh with 136664 triangles and 69253 nodes. Time steps were $1/6400$ (2-SBDF) and 1×10^{-8} (1-SBDF). Initial data was prescribed as perturbations of the stationary solutions (see text for further details). The schematic mammal skin domains are bounded by rectangles with the following dimensions: **a** 0.5×0.75, **b** 8×12, **c** 32×48, **d** 128×192

$$u_0(x, y) = u_c(1 + \widehat{p}(x, y)/10),$$
$$v_0(x, y) = v_c(1 + \widehat{p}(x, y)/10),$$

i.e., the stationary states are perturbed up to a maximum of $\pm$ 10%.

We solved the schemes until the transient solutions died out ($T = 500$), and checked that the solutions were unchanged at $t = 2T$, which confirmed that the patterns represented stationary solutions. In order to verify that the patterns represented correctly converged solutions we also checked that solutions were unchanged with refinement of the spatial and temporal discretization parameters. In all calculations we used the unstructured mesh generator MESH2D (v24).[1]

[1] See http://www.mathworks.com/matlabcentral/fileexchange/ for further details.

4.1.2 Rates of convergence

We present numerical evidence in two space dimensions to test the optimal rate of convergence given in Theorem 4. As no exact solution of the reaction-diffusion system is known, we compared approximate solutions u^n computed with a small time step Δt_{fine}, with the corresponding solutions U^n generated with a sequence of larger time steps $\{\Delta t\}$. In all simulations we used a fine triangulation $\mathcal{T}^h$ with a maximum diameter of all triangles equal to h (additional details below).

For notational convenience we extend the approximate solutions in time via

$$\begin{aligned} u^+(t) &:= u^n, \quad t \in (t_{n-1}, t_n], \quad t_n := n\Delta t_{\text{fine}}, \quad n = 1, 2, \ldots, N_{\text{fine}}, \\ U^+(t) &:= U^n, \quad t \in (t_{n-1}, t_n], \quad t_n := n\Delta t, \quad n = 1, 2, \ldots, N, \\ N_{\text{fine}} &:= T/\Delta t_{\text{fine}}, \quad N := T/\Delta t, \end{aligned}$$

and define the errors

$$\begin{aligned} \eta_0(h, \Delta t) &:= \|u^+ - U^+\|^2_{L^2(0,T;H^1(\Omega))} = \Delta t \sum_{n=1}^{N} \left(\|u^n - U^n\|_0^2 + |u^n - U^n|_1^2 \right), \\ \eta_\infty(h, \Delta t) &:= \|u^+ - U^+\|^2_{L^\infty(0,T;L^2(\Omega))} = \max_{1 \le n \le N} \|u^n - U^n\|_0^2. \end{aligned}$$

Using *Lumped Mass Qaudrature* ([24, p. 340]) we computed the ratios

$$R_i^{\Delta t} := \frac{\eta_i(h, \Delta t) - \eta_i(h, \Delta t/2)}{\eta_i(h, \Delta t/2) - \eta_i(h, \Delta t/4)}, \quad i = 0, \infty, \tag{4.5}$$

for a typical example computed in Sect. 4.1.1 (see Table 1 for additional details). With the assumption that $\eta_0(h, \Delta t)$ and $\eta_\infty(h, \Delta t)$ can be expressed in the form $C_1 h^p + C_2 \Delta t^q, \quad p, q, C_1, C_2 \in \mathbb{R}$, the ratios (4.5) simplify to $R_0^{\Delta t} = R_\infty^{\Delta t} = 2^q$. Thus the results in Table 1 indicate that the rate of convergence is $\mathcal{O}(\Delta t^2)$, which is consistent with the error bound in Theorem 4.

Table 1 Verification of Theorem 4: $\Delta t_{\text{fine}} = 1/12800$; $h = 0.003$; $Lx = 1$; $Ly = 1.5$; $\Delta t = 2^{-j}/25$, $j = 0, 1, \ldots, 7$

Δt	$\eta_0(3/1000, \Delta t)$	$\eta_\infty(3/1000, \Delta t)$	$R_0^{\Delta t}$	$R_\infty^{\Delta t}$
1/25	7.920e−02	2.098e−04	3.05	2.07
1/50	2.473e−02	7.242e−05	3.52	3.26
1/100	6.687e−03	2.163e−05	3.77	3.50
1/200	1.180e−03	6.033e−06	3.92	3.76
1/400	4.550e−04	1.582e−06	4.02	3.92
1/800	1.116e−04	3.972e−07	4.15	4.08
1/1600	2.631e−05	9.495e−08	–	–
1/3200	5.750e−06	2.091e−08	–	–

For details concerning the initial data and other parameter values see Sect. 4.1.1

5 Conclusions

We studied a second-order, three level finite element approximation of a well-known reaction-diffusion ('Thomas') system for patterning in nature. For the spatial discretization we used the standard Galerkin finite element method with piecewise linear continuous basis functions. For the temporal discretization we employed the second-order 2-SBDF finite difference scheme, with starting values computed from the first-order 1-SBDF scheme [55]. The main contribution of this paper is the numerical analysis of the semi-discrete in time weak formulation of the Thomas system. The three time levels of the scheme and the asymmetry of the approximate reaction-kinetics presents significant technical challenges for the derivation of *a priori* estimates and the optimal semi-discrete in time error estimate. To the best of our knowledge, our study provides the first comprehensive numerical analysis of a multi-level (≥ 3) semi-discrete in time weak formulation for a system of nonlinear reaction-diffusion equations.

The methodology in this paper shows promise in the numerical analysis of the Extrapolated Gear scheme (1.4) applied to other reaction-diffusion systems. The analysis should cover reaction-diffusion systems where the reaction-kinetics satisfy Lemma 4 and a local Lipschitz condition (see Lemma 1). Further work is needed to generalize the numerical analysis to cover systems that do not satisfy these lemmata. However, much of our work deals with discrete energy estimates of the three level time derivative, and is therefore applicable to general systems of semi-linear PDEs.

In order to illustrate the numerical performance of the finite element method studied in this paper, we repeated an experiment of Murray [44] (see also [45]), who simulated Turing patterns over a schematic mammal skin with fixed geometry and various domain sizes. This is a classic experiment in mathematical biology, and the numerical results have been reproduced in numerous sources, e.g. [20,21,47].[2] However, in Murray's original work insufficient details were given for the numerical simulations to be accurately duplicated. Furthermore, the traditional approach used to prescribe initial data for diffusion-driven instability is also not repeatable. Typically with this approach, the spatially homogeneous equilibrium solutions are perturbed at every point on the computational grid, using an unspecified random number generator with an unspecified 'seed' value. As the numerical solution is sensitive to small changes in the initial and boundary data [6], even results obtained with the same random number generator, but with different 'seeds', vary significantly. Another problem with this procedure is that mesh refinement cannot be used to demonstrate convergence, as successive grids necessitate the use of essentially *different* initially conditions. To overcome these problems we provided a consistent procedure for generating initial data that can be used to generate Turing patterns, which is useful for future comparative work using the Thomas system, or other Turing systems.

We hope the work in this paper stimulates additional numerical analysis of multi-level finite element schemes for nonlinear reaction-diffusion systems.

Acknowledgments We thank James Blowey (University of Durham, UK) for some helpful comments during the preparation of this manuscript and for the comments of the anonymous reviewers.

[2] The physics review paper [20] has been cited 4068 times (ISI Web of Knowledge).

Appendix: Pseudo random number generation

In the interests of repeatability, we give details of the pseudo random number generator D_UNIFORM_01 [37] used to perturb the coefficients z_{rs} of the double Fourier series (4.4). It is not the most efficient random number generator, but it is simple enough to be easily implemented in different languages.

We take z_{rs} equal to the nth random number r_n drawn from D_UNIFORM_01, where $n = r + 20(s - 1)$. The random numbers are calculated recursively via

$$r_n = s_n/(2^{31} - 1),$$
$$s_n = 16807 * s_{n-1} * \mod (2^{31} - 1),$$

for $n = 1, 2, \ldots$ 'seeded' with s_0. In all our simulations we used $s_0 = 4$.

References

1. Akrivis, G., Crouzeix, M.: Linearly implicit methods for nonlinear parabolic equations. Math. Comp. **73**(246), 613–635 (2003)
2. Akrivis, G., Crouzeix, M., Makridakis, C.: Implicit–explicit multistep finite element methods for nonlinear parabolic problems. Math. Comput. **67**(222), 457–477 (1998)
3. Akrivis, G., Crouzeix, M., Makridakis, C.: Implicit–explicit multistep methods for quasilinear parabolic equations. Numer. Math. **82**, 521–541 (1999)
4. Akrivis, G., Smyrlis, Y.-S.: Implicit–explicit BDF methods for the Kuramoto-Sivashinsky equation. Appl. Numer. Math. **51**, 151–169 (2004)
5. Apostol, T.M.: Mathematical Analysis, 2nd edn. Addison-Wesley Publishing Co., Reading (1974)
6. Arcuri, P., Murray, J.D.: Pattern sensitivity to boundary and initial conditions in reaction-diffusion models. J. Math. Biol. **24**, 141–165 (1986)
7. Ascher, U.M., Ruuth, S.J., Wetton, B.T.R.: Implicit-explicit methods for time-dependent partial differential equations. SIAM J. Numer. Anal. **32**(3), 797–823 (1995)
8. Attouch, H., Buttazzo, G., Michaille, G.: Variational Analysis in Sobolev and BV Spaces: Applications to PDEs and Optimization. Mps-Siam Series on Optimization, vol. 6. SIAM, Philadelphia (2006)
9. Ball, J.M.: Remarks on blow-up and nonexistence theorems for nonlinear evolution equations. Q. J. Math. Oxford **2**(28), 473–486 (1977)
10. Barrett, J.W., Blowey, J.F.: An error bound for the finite element approximation of the Cahn-Hilliard equation with logarithmic free energy. Numer. Math. **72**, 1–20 (1995)
11. Bramble, J.H., Pasciak, J.E., Sammon, P.H., Thomée, V.: Incomplete iterations in multistep backward difference methods for parabolic problems with smooth and nonsmooth data. Math. Comp. **52**(186), 339–367 (1989)
12. Ceniceros, H.D.: A semi-implicit moving mesh method for the focusing nonlinear Schrödinger equation. Commun. Pure Appl. Anal. **1**(4), 1–14 (2002)
13. Chen, W.: Implicit–explicit multistep finite element methods for nonlinear convection-diffusion problems. Numer. Methods Partial Differ. Equ. **17**(2), 93–104 (2001)
14. Chen, W.: Implicit-explicit multistep finite element methods for a semiconductor device with heat conduction. J. Math. Study **35**(2), 109–123 (2002)
15. Chen, W.: Implicit-explicit multistep finite element methods for the semiconductor device problem. J. Syst. Sci. Complex. **16**(1), 101–113 (2003)
16. Chen, W.: Implicit-explicit multistep finite element mixed finite element methods for the transient behavior of a semiconductor device. Acta Math. Sci. Ser. B Engl. Ed. **3**, 386–398 (2003)
17. Chueh, K.N., Conley, C.C., Smoller, J.A.: Positively invariant regions for systems of nonlinear diffusion equations. Indiana Univ. Math. J. **26**(2), 373–392 (1977)
18. Ciarlet, P.G.: The Finite Element Method for Elliptic Problems. In: Studies in Mathematics and its Applications, vol. 4. North-Holland, Amsterdam (1979)

19. Crank, N., Nicolson, P.: A practical method for numerical evaluation of solutions of partial differential equations of the heat conduction type. Proc. Camb. Phil. Soc. **43**, 50–67 (1947)
20. Cross, M.C., Hohenberg, P.C.: Pattern formation outside of equilibrium. Rev. Modern Phy. **65**(3), 851–1060 (1993)
21. Edelstein-Keshet, L.: Mathematical Models in Biology. Classics in Applied Mathematics, vol. 46. Society for Industrial and Applied Mathematics (SIAM), Philadelphia (2005)
22. Elliott, C.M., Stuart, A.M.: The global dynamics of discrete semilinear parabolic equations. SIAM J. Numer. Anal. **30**(6), 1622–1663 (1993)
23. Emmrich, E.: Stability and error of the variable two-step BDF for semilinear parabolic problems. J. Appl. Math. Comput. **19**(1–2), 33–55 (2005)
24. Eriksson, K., Estep, D., Hansbo, P., Johnson, C.: Computational Differential Equations. Cambridge University Press, Cambridge (1996)
25. Ethier, M., Bourgault, Y.: Semi-implicit time-discretization schemes for the bidomain model. SIAM J. Numer. Anal. **46**(5), 2443–2468 (2008)
26. Frank, J., Hundsdorfer, W., Verwer, J.G.: On the stability of implicit-explicit linear multistep methods. Appl. Numer. Math. **25**, 193–205 (1997)
27. Garvie, M.R.: Analysis of a Reaction-Diffusion System of $\lambda - \omega$ type. University of Durham, PhD thesis (2003)
28. Garvie, M.R., Blowey, J.F.: A reaction-diffusion system of $\lambda - \omega$ type. Part II: Numerical analysis. Eur. J. Appl. Math. **16**(5), 621–646 (2005)
29. Garvie, M.R., Trenchea, C.: Finite element approximation of spatially extended predator-prey interactions with the Holling type II functional response. Numer. Math. **107**, 641–667 (2007)
30. Henry, D.: Geometric Theory of Semilinear Parabolic Equations. In: Lecture Notes in Mathematics, vol. 840. Springer, New York (1981)
31. Holden, A.V., Markus, M., Othmer, H.G. (eds.): Nonlinear Wave Processes in Excitable Media. Plenum, New York (1991)
32. Hollis, S.L., Martin, R.H., Pierre, M.: Global existence and boundedness in reaction-diffusion systems. SIAM J. Math. Anal. **18**(3), 744–761 (1987)
33. Hundsdorfer, W., Verwer, J.: Numerical solution of time-dependent advection-diffusion-reaction equations. In: Springer Series in Computational Mathematics, vol. 33. Springer, Berlin (2003)
34. Keller, E.F., Segel, L.A.: Travelling bands of bacteria: a theoretical analysis. J. Theor. Biol. **30**, 235–248 (1971)
35. Layton, W., Trenchea, C.: Stability of two IMEX methods, CNLF-AB2, for uncoupling systems of evolution equations. Appl. Numer. Math. **62**(2), 112–120 (2012)
36. Levin, S.A., Segel, L.A.: Hypothesis for origin of plankton patchiness. Nature **259**, 659 (1976)
37. Lewis, P., Goodman, A., Miller, J.: A pseudo-random number generator for the system/360. IBM Syst. J. **8**(2), 136–143 (1969)
38. Li, D., Zhang, C., Wang, W., Zhang, Y.: Implicit-explicit predictor-corrector schemes for nonlinear parabolic differential equations. Appl. Math. Model. **35**, 2711–2722 (2011)
39. Lubich, C., Ostermann, A.: Runge-Kutta time discretization of reaction-diffusion and Navier-Stokes equations: nonsmooth-data error estimates and applications to long-time behaviour. Appl. Numer. Math. Trans. IMACS **22**(1–3), 276–292 (1996)
40. Madzvamuse, A.: Time-stepping schemes for moving grid finite elements applied to reaction-diffusion systems on fixed and growing domains. J. Comput. Phys. **214**, 239–263 (2006)
41. Maini, P.K.: Using mathematical models to help understand biological pattern formation. C. R. Biol. **327**, 225–234 (2004)
42. Medvinsky, A.B., Petrovskii, S.V., Tikhonova, I.A., Malchow, H., Li, B.-L.: Spatiotemporal complexity of plankton and fish dynamics. SIAM Rev. **44**(3), 311–370 (2002)
43. Moore, P.: Finite element multistep multiderivative schemes for parabolic equations. J. Inst. Math. Appl. **21**, 331–334 (1978)
44. Murray, J.D.: On pattern formation mechanisms for lepidopteran wing patterns and mammalian coat markings. Phil. Trans. R. Soc. Lond. B **295**, 473–496 (1981)
45. Murray, J.D.: On pre-pattern formation mechanism for animal coat markings. J. Theor. Biol. **88**, 161–199 (1981)
46. Murray, J.D.: Parameter space for turing instability in reaction diffusion mechanisms: a comparison of models. J. Theor. Biol. **98**, 143–163 (1982)
47. Murray, J.D.: Mathematical biology. Biomathematics Texts, vol. 19. Springer, Berlin (1993)

48. Nie, Y.-Y., Thomeé, V.: A lumped mass finite-element method with quadrature for a non-linear parabolic problem. IMA J. Numer. Anal. **5**, 371–396 (1985)
49. Ochoa, F.L., Murray, J.D.: A non-linear analysis for spatial structure in a reaction-diffusion model. Bull. Math. Biol. **45**(6), 917–930 (1983)
50. Pazy, A.: Semigroups of Linear Operators and Applications to Partial Differential Equations. Applied Mathematical Sciences, vol. 44. Springer, New York (1983)
51. Piotrowska, M.J.: Activator-inhibitor system with delay and pattern formation. Math. Comput. Modelling **42**(1–2), 123–131 (2005)
52. Quarteroni, A.: Numerical models for differential problems. In: MS&A. Modeling, Simulation and Applications, vol. 2. Springer, Milan (2009)
53. Quarteroni, A., Sacco, R., Saleri, F.: Numerical mathematics. Texts in Applied Mathematics, vol. 37, 2nd edn. Springer, Berlin (2007)
54. Rionero, S., Vitiello, M.: Long-time behavior of the solutions of Murray–Thomas model for interacting chemicals. Math. Comput. Simul. **82**, 1597–1614 (2012)
55. Ruuth, J.R.: Implicit-explicit methods for reaction-diffusion problems in pattern formation. J. Math. Biol. **34**, 148–176 (1995)
56. Sgura, I., Bozzini, B., Lacitignola, D.: Numerical approximation of Turing patterns in electrodeposition by ADI methods. J. Comput. Appl. Math. **236**, 4132–4147 (2012)
57. Temam, R.: Infinite-dimensional dynamical systems in mechanics and physics. In: Applied Mathematical Sciences, vol. 68. Springer, New York (1997)
58. Thomas, D.: Artificial enzyme membranes, transport, memory and oscillatory phenomena. In: Thomas, D., Kernevez, J.P. (eds.) Analysis and Control of Immobilized Enzyme Systems, pp. 115–150. Springer, Berlin (1975)
59. Thomas, J.W.: Numerical partial differential equations: finite difference methods. In: Texts in Applied Mathematics, vol. 22. Springer, New York (1995)
60. Turing, A.M.: The chemical basis of morphogenesis. Phil. Trans. R. Soc. Lond. B **237**, 37–72 (1952)
61. Varah, J.M.: Stability restrictions on second order, three level finite difference schemes for parabolic equations. SIAM J. Numer. Anal. **17**(2), 300–309 (1980)
62. Zhang, K., Wong, J.C.-F., Zhang, R.: Second-order implicit-explicit scheme for the Gray-Scott model. J. Comput. Appl. Math. **213**, 559–581 (2008)
63. Zlámal, M.: Finite element multistep discretizations of parabolic boundary value problems. Math. Comp. **29**(130), 350–359 (1975)